Design, syntheses, and characterization of dioxo-molybdenum(VI) complexes with thiolate ligands: effects of intraligand NH · · · S hydrogen bonding

Raghvendra S. Sengar, Jonathan J. Miller and Partha Basu*

Received 18th September 2007, Accepted 28th February 2008
First published as an Advance Article on the web 27th March 2008
DOI: 10.1039/b714386a

Presence of the hydrogen bonding near a metal center can influence the properties of the complex. Here, we describe changes in redox and spectral properties in discrete dioxo-molybdenum centers coordinated by a single thiolato ligand that can support an intra-ligand hydrogen bond. We have utilized thiophenolato ligands that can harbor hydrogen bonding between the thiophenolato sulfur with an amide functionality creating either a five- or a six-membered ring. Methylation of the amide functionality removes the NH · · · S hydrogen bonding thus providing a basis for understanding the effect of hydrogen bonding. These thiophenolato ligands have been used in synthesizing dioxo-Mo^{VI} complexes of type $Tp^*MoO_2(S\text{-}o\text{-}RC_6H_4)$, where R = CONHMe (**11**), $CONMe_2$ (**12**), NHCOMe (**13**), and N(Me)COMe (**14**). The complexes have been characterized by NMR, infrared, and UV-visible spectroscopy. Spectroscopic data clearly indicate the presence of hydrogen bonding in both **11** and **13**, and stronger in **13**, where hydrogen bonding stabilizes a five-membered ring. All complexes exhibit a Mo^{VI}/Mo^{V} redox couple and redox potentials are modulated by the nature of H-bonding. Compound **14** with the electron-releasing N(Me)COMe group has the highest reduction potential and is more difficult to reduce.

Introduction

The presence of hydrogen bonding is extensive in biological systems.[1] It plays important roles in the functioning of biological molecules such as structural organization, control of redox potential, substrate entry and product release. Hydrogen bonding is ubiquitous in metalloenzymes including mononuclear molybdenum enzymes which carry out many essential life processes.[2] We are interested in understanding how hydrogen bonding can influence the redox properties of oxo-molybdenum centers, which are the active centers of mononuclear molybdenum enzymes. Extended hydrogen bonding constitutes catalytic pockets often creating a positively charged channel conducive to binding of anionic product or substrate. For example, in the active site of sulfite oxidase (SO), a network of H-bonded water molecules from SO_3^{2-} to the oxomolybdenum center has been observed,[3–6] which raises questions about the roles of hydrogen bonding in modulating properties of the metal center. Sulfite oxidase is considered to be a prototypical oxotransferase, where water serves as the ultimate source of oxygen atom.[7] A simplified view of the reductive half cycle of sulfite oxidase is shown in Fig. 1, where a water molecule is hydrogen bonded to the substrate (sulfite). In this model, the product (sulfate) is generated *via* electron- and proton-transfer processes.

Synthetic models of molybdenum enzymes generally use two main approaches for introducing hydrogen bonding—one that harbors H-bonding within the ligand, and one where H-bonding involves an anion, cation or a solvent molecule.[8–10] Both approaches have been successfully utilized in developing models for molybdenum enzymes. We are primarily interested in the former approach, where a hydrogen-bonding unit is placed by design. Several synthetic models for the oxo-molybdenum center of molybdoenzymes have been synthesized, where the ligand provides one or more hydrogen-bonded unit(s) in close proximity to a metal center. This proximity strongly influences the properties of the metal center. Much emphasis has been given to the 5-membered, 2-(acylamino)benzene thiolate ligands (type B, Fig. 2), which exhibited a large positive shift in redox potential in alkylammonium salts of $[Mo^{V}O(S\text{-}o\text{-}R'CONHC_6H_4)_4$[11,12] and $[Mo^{IV}O\{1,2\text{-}S_2\text{-}3,6\text{-}(R'CONH)_2C_6H_2\}_2]$ (R′ = CH_3, CF_3, *t*-Bu, Ph_3C).[13,14] The effect of intramolecular hydrogen bonding was evaluated by comparing the corresponding *N*-methylated complexes where such hydrogen bonding is not present. The sensitivity of the redox potential to similar hydrogen bonding has been reported for the molybdenum nitrosyl compound, $Tp^*Mo(NO)(SCH_2CONHCH_3)_2$.[15] Several other metals such as tungsten,[16] iron,[17] zinc,[18] cadmium,[18d,19] mercury,[20] cobalt,[21] copper,[22] platinum and palladium[23] have also been reported to form a complex with 2-(acylamino)benzene thiolate-type ligands. In these complexes, various thiolato ligands have an influence on the properties of the metal center. The presence of a NH · · · S hydrogen bond not only contributes to the positive shifts in the redox potentials in complexes, but also affects their spectral and structural properties by modulating the metal–sulfur interaction.

2-(Alkylcarbamoyl)benzene thiolate ligands (type A, Fig. 2) constitute a different class of ligands, which can potentially exhibit intramolecular hydrogen bonding such as SH · · · O=C or S · · · HN in protonated thiol forms or in deprotonated thiolato forms respectively. While such units have not been fully explored in oxo-molybdenum chemistry, their mercury, platinum, palladium, iron and gallium complexes have been reported.[23–25] These

Department of Chemistry and Biochemistry, Duquesne University, Pittsburgh, PA, 15282, USA. E-mail: basu@duq.edu

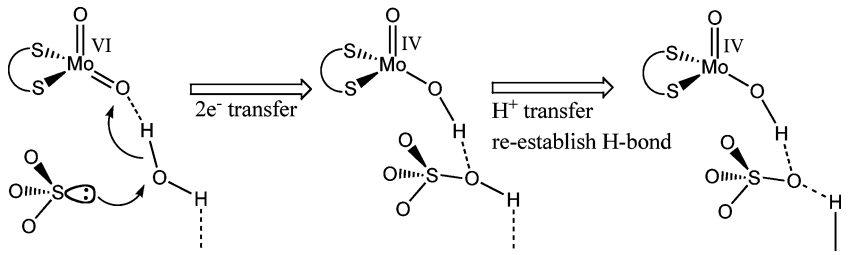

Fig. 1 Transfer of an oxygen atom from the H-bonded remote second-coordination-sphere water molecule to oxidizing sulfite to sulfate.[7]

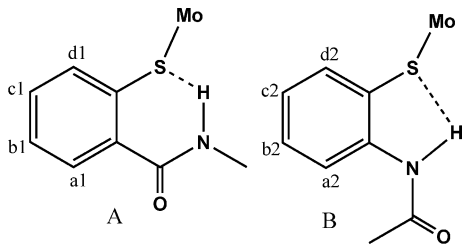

Fig. 2 Two modes of intra-ligand NH · · · S hydrogen bonding used in this investigation.

complexes, *e.g.* [Pt(bpy)(S-*o*-MeNHCOC$_6$H$_4$)$_2$] and (NEt$_4$)$_2$[Hg(S-*o*-MeNHCOC$_6$H$_4$)$_4$], possess weak NH · · · S intra-ligand (type A) hydrogen bonding.[23,24] In the alkyl analogue of type A thiolates, based on infrared studies Zuppiroli *et al.* have proposed extended structures of the neutral HSC$_2$H$_4$CONHCH$_3$ ligand.[26] This was also found in Tp*Mo(NO)(S(CH$_2$)$_2$CONHCH$_3$)[15], where no six-membered cyclic structure containing S · · · HN was found in its crystal structure. Instead, an interligand O · · · HN was observed. Interestingly, complexes like Tp*Mo(NO)(S(CH$_2$)$_2$CONHCH$_3$) and Tp*Mo(NO)(S(CH$_2$)$_2$CONH(CH$_2$)$_2$S)[27] do not possess an intra-ligand H-bond but their redox potentials are shifted towards higher values compared to the *N*-methylated complexes.

Herein we report the syntheses and characterization of dioxomolybdenum complexes with ligands harboring type A and type B hydrogen-bonding units. In addition, we also report the syntheses and characterization of complexes of the corresponding *N*-methylated ligands that cannot exhibit similar hydrogen bonding. We demonstrate that in both types (type A and type B) H-bonding can influence the spectral as well as the electrochemical properties of the complexes.

Experimental

Unless otherwise specified, all the reactions were carried out in oven-dried glassware in dry atmospheres of argon using standard Schlenk techniques. All work-up and chromatographic purifications of complexes were conducted in air using distilled solvents. Solvents were purified as follows: dichloromethane (CH$_2$Cl$_2$) from CaH$_2$; toluene, hexane and tetrahydrofuran (THF) from Na-benzophenone; ethanol (EtOH) by refluxing with freshly prepared sodium ethoxide. Triethylamine and pyridine were purified by distilling over KOH pellets. For adsorption chromatography, silica gel (60 Å, 63–200 μm) from Sorbent Technologies was used. Thin-layer chromatography (TLC) was performed on silica-gel-coated plastic plates also purchased from Sorbent Technologies.

Room temperature ^{1}H and ^{13}C NMR spectra were recorded using a Bruker ACP-300 spectrometer at 300.133 MHz and 75.469 MHz frequencies respectively. Additional ^{1}H NMR spectra were collected on a Bruker 400 MHz spectrometer. Deuterated solvents were obtained from Cambridge Isotope laboratories and were used without further purification. Solid-state infrared spectra were recorded on a Perkin-Elmer FT-IR 1760X spectrometer in KBr pellets. Solution IR spectra were recorded using a flow through CaF$_2$ cell with 0.1 mm solvent path length. Mass spectra were collected on Micromass ZMD mass spectrometer using both negative and positive ionization modes. Acetonitrile (or methanolic) solutions of the samples were injected *via* a syringe pump with a flow rate of 0.1–0.2 ml min^{-1}. Electronic spectra of complexes were collected on a Cary 3 spectrophotometer. Cyclic voltammograms (CVs) of complexes were recorded on a Bioanalytical systems (BAS) model CV-50W using a standard three-electrode system, consisting of Pt-disk working and reference electrodes and a Pt-wire auxiliary electrode. Measurements were performed in dry and degassed acetonitrile using 0.2M NBu$_4$ClO$_4$ of supporting electrolyte, and internally referenced with an Fc$^+$/Fc couple, and the potentials are expressed with respect to the Fc$^+$/Fc couple.

Synthesis

Tp*MoO$_2$Cl and Tp*MoO$_2$(SPh) were prepared following the published methods.[28] Similarly, *N*-[2-(2-acetylaminophenyldisulfanyl)phenyl]acetamide, **7**, and *N*-{2-[2-(acetylmethylamino)-phenyldisulfanyl]phenyl}-*N*-methylacetamide, **8**, were synthesized according to the literature procedure.[29]

2,2′-Disulfanediyldibenzoic acid, 1. To a solution of 2-mercapto benzoic acid (1.5 g, 9.74 mmoles) in 95% EtOH (100 ml) was added a saturated solution of I$_2$ in 95% EtOH in an open atmosphere until a light-yellow color of the reaction mixture persisted. Precipitation of a white solid occurred after ~30 min of stirring, which was collected and washed with ethanol. Solid was further dried under vacuum at 50 °C. Yield, 60% (0.9 g, 2.94 mmoles). NMR (^{1}H, δ/ppm) in (CD$_3$)$_2$SO: 7.33 (t, 2H, J = 7.3 Hz,); 7.55 (t, 2H, J = 7.3 Hz); 7.62 (d, 2H, J = 8.1 Hz); 8.02 (d, 2H, J = 7.5 Hz). NMR (^{13}C, δ/ppm) in (CD$_3$)$_2$SO: 125.04; 125.96; 128.12; 131.55; 133.21; 138.93; 167.58. IR (KBr, cm^{-1}): 2920, 2661, 1683, 1587, 1561, 1461, 1416, 1310, 1292, 1260, 1151, 1056, 1038, 898, 809, 738, 695, 651. ESI$^-$-MS (CH$_3$OH): m/z: 153.03 [1/2(M − 2H)]$^{2-}$, (M = C$_{14}$H$_{10}$O$_4$S$_2$, 306.36).

2-Chlorocarbonyl-phenyl disulfanyl benzyl chloride, 2. To a mixture of **1** (3 g, 9.8 mmoles) and *N*,*N*-dimethylformamide (1 ml) in THF (25 ml) was slowly added oxalyl chloride (8.5 ml, 97.4 mmoles) at 0 °C. The reaction mixture was gradually warmed to room temperature and further stirred for 3 h. Evaporation of solvents to dryness under reduced pressure afforded a yellow solid in quantitative yield which was characterized without further purifications. NMR (^{1}H, δ/ppm) in $(CD_3)_2SO$: $\delta = 7.39$ (t, 2H, $J =$ 7.2 Hz); 7.55 (t, 2H, $J = 7.6$ Hz); 7.76 (d, 2H, $J = 9.1$ Hz); 8.38 (d, 2H, $J = 7.8$ Hz). NMR (^{13}C, δ/ppm) in $(CD_3)_2SO$: 126.18; 126.44; 130.46; 135.12; 135.60; 141.55; 167.50. IR (KBr, cm^{-1}): 1718, 1583, 1555, 1446, 1435, 1199, 1133, 1039, 898, 879, 764, 721, 695, 655.

2,2′-Disulfanediylbis(*N*,*N*-dimethylbenzamide), 3. A solution of freshly prepared **2** (3.36 g, 9.8 mmoles) in CH_2Cl_2 (30 ml) was slowly added to a mixture of $MeNH_2$·HCl (2.0 g, 29.6 mmoles) and Et_3N (8.2 ml, 58.9 mmoles) in CH_2Cl_2 (15 ml) at 0 °C. The reaction mixture was gradually warmed to room temperature and stirred overnight. The reaction was quenched with water and a white precipitate was filtered, washed with water and dried in a desiccator. Yield, 75% (2.44 g, 7.35mmoles). NMR (^{1}H, δ/ppm) in $(CD_3)_2SO$: 2.73 (d, 6H, $J = 4.3$ Hz); 7.30 (t, 2H, $J = 7.4$ Hz); 7.45 (t, 2H, $J = 7.3$ Hz); 7.63 (m, 4H); 8.58 (m, 2H). This compound was sparingly soluble in $CHCl_3$. NMR (^{1}H, δ/ppm) in $CDCl_3$ 2.99 (d, 6H, $J = 4.8$ Hz), 6.16 (s, 2H), 7.25 (t, $J = 7.3$ Hz), 7.37 (t, 2H, $J = 8.0$ Hz), 7.48 (d, 2H, $J = 7.7$ Hz), 7.76 (d, 2H, $J = 7.8$ Hz). NMR (^{13}C, δ/ppm) in $(CD_3)_2SO$: 26.18; 125.85; 127.80; 131.04; 133.71; 136.64; 167.24. IR (KBr, cm^{-1}): 3284, 3084, 1632, 1551, 1406, 1327, 745, 695. ESI$^+$-MS (CH_3CN): m/z: 333.31 $[M + H]^+$, ($M = C_{16}H_{16}N_2O_2S_2$, 332.07).

2-(Dimethylcarbamoyl-phenyldisulfanyl)-*N*,*N*-dimethyl benzamide, 4. This compound was synthesized by following the procedure described for **3** using compound **2** (4.48 g, 13.06 mmoles), Me_2NH·HCl (3.26 g, 40 mmoles), and Et_3N (11.0 ml, 79.5 mmoles) in CH_2Cl_2 (50 ml). After the addition of water, the organic layer was separated, dried over anhydrous $MgSO_4$ and evaporated to yield a light-pink solid, which was further purified by a silica column using a 5–30% gradient of acetonitrile in toluene. Yield, 80% (3.77 g, 10.45 mmoles). NMR (^{1}H, δ/ppm) in CD_3CN: 2.74 (s, 6H); 3.05 (s, 6H); 7.24 (d, 2H, $J = 7.4$ Hz); 7.34 (t, 2H, $J = 7.3$ Hz); 7.41 (t, 2H, $J = 7.8$ Hz), 7.73 (d, 2H, $J = 7.7$ Hz). NMR (^{13}C, δ/ppm) in CD_3CN: 22.06; 35.98; 127.19; 128.40; 128.67; 129.41; 135.26; 141.65; 165.8. NMR (^{1}H, δ/ppm) in $CDCl_3$: 2.84 (s, 6H); 3.12 (s, 6H); 7.20 (d, 2H, $J = 7.0$ Hz); 7.26 (t, 2H, $J = 7.2$ Hz); 7.33 (t, 2H, $J = 7.4$ Hz); 7.68 (d, 2H, $J = 7.2$ Hz). NMR (^{13}C, δ/ppm) in $CDCl_3$: 35.00; 38.90; 127.01; 127.64; 128.83; 130.03; 134.24; 136.75; 169.39. IR (KBr, cm^{-1}): 3049, 2926, 1648, 1620, 1586, 1508, 1392. ESI$^+$-MS (CH_3CN): m/z: 360.1 $[M + H]^+$, ($M = C_{18}H_{20}N_2O_2S_2$, 360.49).

2-Mercapto *N*-methyl benzamide, 5. To a solution of **3** (1.65 g, 1.99 mmoles) in EtOH (20 ml) and THF (20 ml) was added $NaBH_4$ (0.30 g, 7.96 mmoles) in small portions at 0 °C and reaction mixture was warmed to room temperature and stirred for 4 h. Solvents were removed under vacuum, the resulting yellow solid was dissolved in distilled water (10 ml) and dilute AcOH was added to acidify the solution to pH ~ 4. A yellowish, oily material separated out from the solution, which was extracted with EtOAc (60 ml) and dried over anhydrous $MgSO_4$. Evaporation of EtOAc yielded a yellow liquid, which was purified by adsorption chromatography on silica gel using a 1 : 3 mixture of acetonitrile and toluene to yield 90% (1.49 g, 3.58 mmoles) of the final product. NMR (^{1}H, δ/ppm) in CD_3CN: 2.84 (d, 3H, $J = 5.8$ Hz); 5.00 (s, 1H); 6.85 (m, 1H); 7.17 (t, 1H, $J = 7.2$ Hz); 7.28 (t, 1H, $J = 7.3$ Hz); 7.35 (d, 1H, $J = 7.2$ Hz); 7.45 (d, 1H, $J = 7.3$ Hz). NMR (^{13}C, δ/ppm) in CD_3CN: 26.69; 126.02; 129.05; 131.50; 134.10; 169.82. IR (KBr, cm^{-1}): 3315, 2936, 2538, 1621, 1588, 1544, 1407, 1319, 1269, 1173, 1042, 1007, 745, 714. ESI$^-$-MS (CH_3CN): m/z: 166 $[M - H]^-$, ($M = C_8H_9NOS$, 167).

2-Mercapto *N*,*N*-dimethyl benzamide, 6. This compound was synthesized by reducing **4** (2.0 g, 5.55 mmoles) with $NaBH_4$ (0.85 g, 22.37 mmoles) in THF–EtOH (12 ml and 12 ml) as described for the synthesis of **5**. Yield, 87.5% (1.75 g, 9.71 mmoles). NMR (^{1}H, δ/ppm) in CD_3CN: 2.83 (s, 3H); 3.09 (s, 3H); 3.74 (s, 1H); 7.15–7.20 (m, 3H); 7.29 (d, 1H, $J = 7.4$ Hz). NMR (^{13}C, δ/ppm) in CD_3CN: 34.57, 38.27; 125.78; 126.71; 128.15; 129.09; 130.69; 136.47; 169.90. IR (KBr, cm^{-1}): 2929, 2515, 1619, 1394. ESI$^-$-MS (CH_3OH): m/z: 180.2 $[M - H]^-$, ($M = C_9H_{11}NOS$, 181.25).

***N*-(2-Mercaptophenyl)acetamide, 9.** This compound was synthesized by reducing the corresponding disulfide, **7** (1.1 g, 3.31 mmoles), following the procedure described for the synthesis of **5** with $NaBH_4$ (0.51 g, 13.4 mmoles) in THF–EtOH (16 ml and 16 ml). Yield, 83% (0.92 g, 5.5 mmoles). NMR (^{1}H, δ/ppm) in CD_3CN: 2.53 (s, 3H); 7.11 (t, 1H, $J = 7.3$ Hz); 7.22 (t, 1H, $J =$ 7.3 Hz); 7.63 (d, 1H, $J = 7.4$ Hz); 7.72 (d, 1H, $J = 7.4$ Hz). NMR (^{13}C, δ/ppm) in CD_3CN: 22.13; 122.45; 122.91; 125.53; 126.73; 136.56; 154.23; 168.09. IR (KBr, cm^{-1}): 3235, 2939, 2546, 1640, 1577, 1528, 1437, 1437, 1298, 1263, 1077, 752. ESI$^-$-MS (CH_3CN): m/z: 166 $[M - H]^-$, ($M = C_8H_9NOS$, 167).

***N*-(2-Mercaptophenyl) *N*-methyl acetamide, 10.** It was synthesized by reducing the corresponding disulfide, **8** (1.5 g, 4.16 mmoles), by following the procedure described for the synthesis of **5** using $NaBH_4$ (0.64 g, 16.84 mmoles) in a THF–EtOH (20 ml and 20 ml) medium. Yield, 95% (1.43 g, 7.90 mmoles). NMR (^{1}H, δ/ppm) in D_2O–$(CD_3)_2SO$: 3.05 (s, 3H); 4.19 (s, 3H); 7.67 (t, 1H, $J = 7.0$ Hz); 7.77 (t, 1H, $J = 7.2$ Hz); 7.97 (d, 1H, $J =$ 7.4 Hz); 8.08 (d, 1H, $J = 7.4$ Hz). NMR (^{13}C, δ/ppm) in D_2O–$(CD_3)_2SO$: 18.07; 37.31; 117.79; 125.16; 129.99; 131.14; 143.07; 177.55. IR (KBr, cm^{-1}): 2415, 1662, 1512, 1462, 1443, 760. ESI$^+$-MS (CH_3CN): m/z: 363.29 $[2M + H]^+$, ($M = C_9H_{11}NOS$, 181.06).

Tp*MoO$_2$(S-*o*-MeNHCOC$_6$H$_4$), 11. A mixture of thiol **5** (0.39 g, 2.34 mmoles) and Et_3N (1 ml, 7.2 mmoles) in CH_2Cl_2 (15 ml) was added to the suspension of Tp*MoO_2Cl (1.10 g, 2.38 mmoles) in CH_2Cl_2 (25 ml) at room temperature and the reaction mixture was stirred for 6 h. Solvent was removed under vacuum and the brown solid residue was chromatographed on silica gel using a mixture of MeCN–toluene (1 : 4). The first brown band was collected and the solvent was evaporated. Yield, 25% (0.35 g, 0.59 mmoles). NMR (^{1}H, δ/ppm) in $CDCl_3$: 2.36 (s, 3H); 2.41 (s, 6H); 2.61 (s, 3H); 2.63 (s, 6H); 2.90 (d, 3H, $J = 4.3$ Hz); 5.86 (s, 3H); 6.62 (m, 1H); 7.11 (t, 1H, $J = 7.3$ Hz); 7.44 (t, 1H, $J =$ 7.5); 7.73 (d, 1H, $J = 7.2$); 8.02 (d, 1H, $J = 8.4$ Hz). NMR (^{13}C, δ/ppm) in $(CD)_3SO$: 12.52; 12.80; 15.09; 15.25, 26.70; 107.34; 107.53; 125.39; 129.23; 130.15; 136.57; 136.95; 140.54; 144.79; 147.2; 153.26; 154.44; 168.95. ESI$^+$-MS (CH_3CN + 0.05%TFA): m/z: 616 $[M + Na]^+$, ($M = C_{23}H_{30}O_3N_7SBMo$, 593).

Tp*MoO$_2$(S-*o*-Me$_2$NCOC$_6$H$_4$), 12. This complex was synthesized using a procedure similar to that described for the synthesis of **11** using Tp*MoO$_2$Cl (1.27 g, 2.74 mmoles), thiol **6** (0.51 g, 2.81 mmoles) and Et$_3$N (1.16 ml, 8.4 mmoles) in CH$_2$Cl$_2$ (45 ml). The reaction mixture was stirred for 18 h. The brown liquid was evaporated to dryness and redissolved in a 1 : 1 mixture of MeCN and toluene and loaded in the silica column. A gradient of MeCN and toluene starting from 10% (MeCN in toluene) was used for purification. Yield, 28% (0.47 g, 0.77 mmoles). NMR (^{1}H, δ/ppm) in CDCl$_3$: 2.36 (s, 6H); 2.39 (s, 3H); 2.65 (s, 9H); 2.83 (s, 3H); 3.03 (s, 3H); 5.86 (m, 3H); 7.15–7.26 (m); 7.42 (m, 1H); 8.1 (d, 1H, J = 7.5). NMR (^{13}C, δ/ppm) in (CD)$_3$SO: 12.95; 13.02; 16.04; 34.80, 38.40; 51.20; 107.44; 124.89; 126.88; 128.75; 129.36; 133.04; 140.50; 169.50. ESI$^+$-MS (CH$_3$CN + 0.05%TFA): m/z: 608 [M + H]$^+$, (M = C$_{24}$H$_{32}$O$_3$N$_7$SBMo, 607).

Tp*MoO$_2$(S-*o*-MeCONHC$_6$H$_4$), 13. This complex was synthesized using a procedure similar to that described for the synthesis of **11** using Tp*MoO$_2$Cl (0.80 g, 1.73 mmoles), thiol **7** (0.36 g, 1.80 mmoles), and Et$_3$N (0.75 ml, 5.4 mmoles) in CH$_2$Cl$_2$ (35 ml). The reaction mixture was stirred for 7 h. Solvent was removed at a reduced pressure and the residue was chromatographed on silica gel using a mixture of MeCN–toluene (1 : 4). The first brown band was collected and the solvent was evaporated to give a solid compound. Yield, 30% (0.31 g, 0.52 mmoles). NMR (^{1}H, δ/ppm) in CDCl$_3$: 2.16 (s, 3H); 2.36 (s, 3H); 2.42 (s, 6H); 2.56 (s, 3H); 2.69 (s, 6H); 5.86 (s, 1H); 5.90(s, 2H); 7.08 (t, 1H, J = 7.3 Hz); 7.18 (t, 1H, J = 7.3); 7.83 (d, 1H, J = 7.3); 8.20 (s, 1H); 8.30 (d, 1H, J = 7.4 Hz). NMR (^{13}C, δ/ppm) in CDCl$_3$: 12.50; 12.76; 15.19; 24.87; 30.82; 107.33; 107.62; 120.01; 123.56; 127.26; 131.56; 134.83; 137.66; 144.96; 147.16; 153.23; 154.26; 168.22. ESI$^+$-MS (CH$_3$CN + 0.05%TFA): m/z: 594 [M + H]$^+$, (M = C$_{23}$H$_{30}$O$_3$N$_7$SBMo, 593).

Tp*MoO$_2$(S-*o*-MeCONMeC$_6$H$_4$), 14. This complex was synthesized using a procedure similar to that described for the synthesis of **12** using Tp*MoO$_2$Cl (1.0 g, 2.16 mmoles), thiol **10** (0.35 g, 1.93 mmoles), and Et$_3$N (0.80 ml, 5.8 mmoles) in CH$_2$Cl$_2$ (40 ml). The reaction mixture was stirred overnight. Solvent was removed at reduced pressure and the residue was chromatographed on silica gel using a mixture of MeCN–toluene (1 : 4). The first brown band was collected and the solvent was evaporated resulting in a solid brown compound. Yield, 18% (0.24 g, 0.39 mmoles). NMR (^{1}H, δ/ppm) in: δ = 1.83 (s, 3H); 2.36 (s, 3H); 2.40 (s, 6H); 2.60 (s, 6H); 2.62 (s, 3H); 3.18 (s, 3H); 5.86–5.92 (m, 3H); 7.22 (d, 1H, J = 7.0 Hz); 7.35 (t, 1H, J = 7.5); 7.45 (t, 1H, J = 7.5); 7.62 (d, 1H, J = 7.6 Hz). NMR (^{13}C, δ/ppm) in (CD)$_3$SO: 7.52; 18.60; 22.05; 58.70, 115.20; 116.10, 140.15; 142.50, 143.22; 150.64; 163.20; 163.92; 164.45; 171.80; 172.50.

Results and discussion

Synthesis and characterization

The functionalized thiol ligands used in this investigation were synthesized by reducing preformed disulfides as outlined in Scheme 1. 2-Mercaptobenzoic acid was oxidized to **1** using I$_2$ in ethanol.[30] Disulfides **3** and **4** were synthesized by modifying a literature procedure,[31] which included first reacting **1** with oxalyl chloride to prepare the acid chloride, **2**, followed by its reaction with MeNH$_2$ or Me$_2$NH. Compound **2** was found to be sensitive to moisture and readily hydrolyzed to **1** upon contact with moisture. Disulfides **3** and **4** were obtained in good yields and were stable in air. Disulfides were reduced to thiol ligands using NaBH$_4$ in THF–ethanol media. Thiols were found to be moderately sensitive towards air and methyl sulfoxide.

Ligands were characterized by solution-phase ^{1}H and ^{13}C NMR spectroscopy and infrared spectroscopy. Due to the low solubility of thiols in chloroform, the NMR spectra were recorded in CD$_3$CN with the exception of compound **10** which was recorded in (CD$_3$)$_2$SO. The aromatic signals of thiols **5**, **6**, **9** and **10** show downfield shifts compared to the corresponding disulfides **3**, **4**, **8** and **9** respectively; however, methyl protons show an opposite upfield shift in thiols compared to the disulfides. The thiols also exhibit a characteristic strong infrared stretch around 2530 cm^{-1} for the S–H group.

Scheme 2 represents the synthetic route to dioxo-Mo^{VI} complexes possessing *ortho*-substituted thiophenol ligands, which follows the ligand substitution reaction similar to Tp*MoO$_2$(SPh). Upon addition of a thiol–Et$_3$N solution into a suspension of Tp*MoO$_2$Cl in CH$_2$Cl$_2$, the reaction mixture changes color from yellow to brown. The progress of the reactions was monitored by thin-layer chromatography (TLC). In general, however, the reactions with substituted ligands took a longer time for completion. Syntheses of complexes **11** and **13** took about 6–7 h, while their methylated partners **12** and **14** required overnight for the reaction to be completed. In all four cases, multiple spots on the TLC plate were observed, indicating side reactions and/or decomposition. Complexes **11–14** were successfully purified by column chromatography over silica gel using a solvent gradient of MeCN in toluene. Complexes **12** and **14**, were further purified by crystallization using toluene and hexane.

The molybdenum complexes were found to be sensitive in solution and to degrade spontaneously releasing the thiophenolato ligand. The sensitivity poses a challenge towards chromatographic separation and contributes to the lower yields. We were unable to obtain suitable quality crystals for structural studies. In fact in most cases we obtained dimeric molybdenum complexes without any thiolato coordination even when we started with spectroscopically (NMR) pure solutions of the complexes. This problem has also resulted in less than optimal elemental analysis of the isolated product. Solutions of the isolated product showed multiple spots on thin-layer chromatography and additional peaks appeared in the NMR spectra.

^{1}H NMR spectroscopy. The ^{1}H NMR spectra of molybdenum complexes have a 2 : 1 ratio for the three-pyrazole methyl groups indicating the C_s local symmetry in solution.[28,30] The amide NH signal in **11** appeared at 6.68 ppm in chloroform-d, which is about 0.52 ppm downfield compared to the NH signal in corresponding disulfide **3** (6.16 ppm in chloroform). Similarly, the amide NH signal in **13** appeared at 8.20 ppm, *i.e.* shifted about 0.30 ppm downfield compared to the corresponding disulfide, **7**.[11] These shifts are consistent with the presence of a H-bond in **11** and **13** as described for other metal complexes.[20–25] Additional support comes from the ^{1}H-NMR spectra of the complexes containing amide –NHCO– and *N*-methylated –NMeCO– moieties. Fig. 3

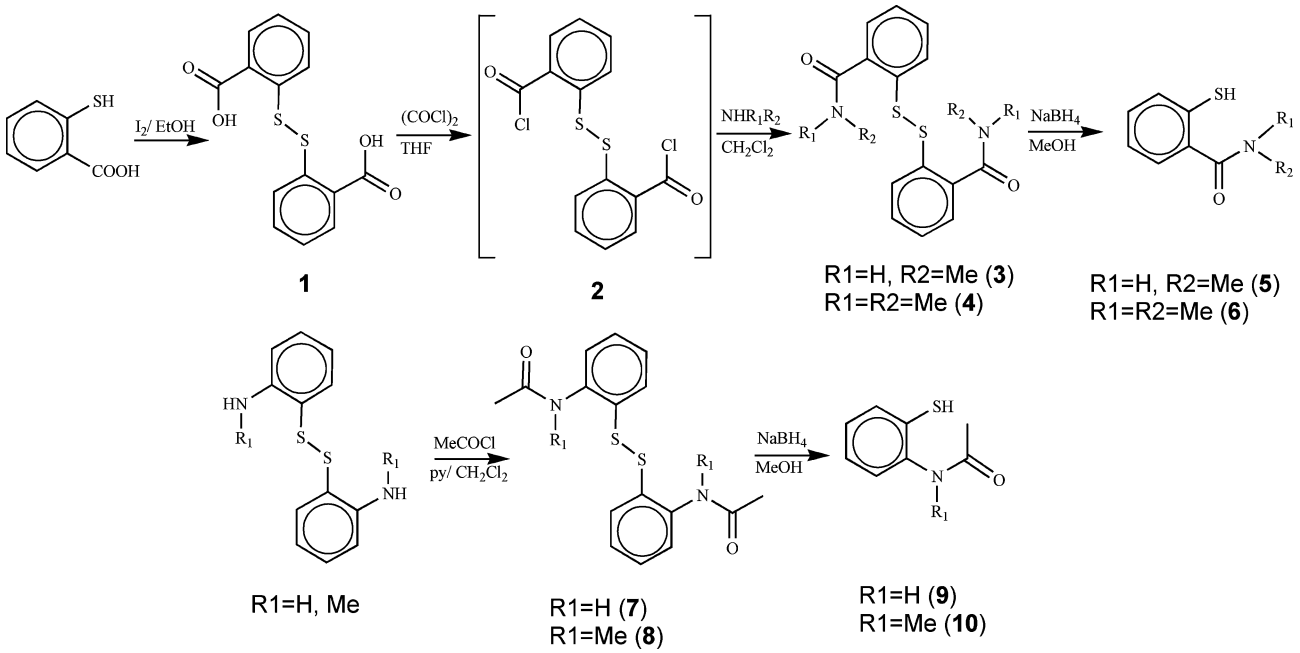

Scheme 1

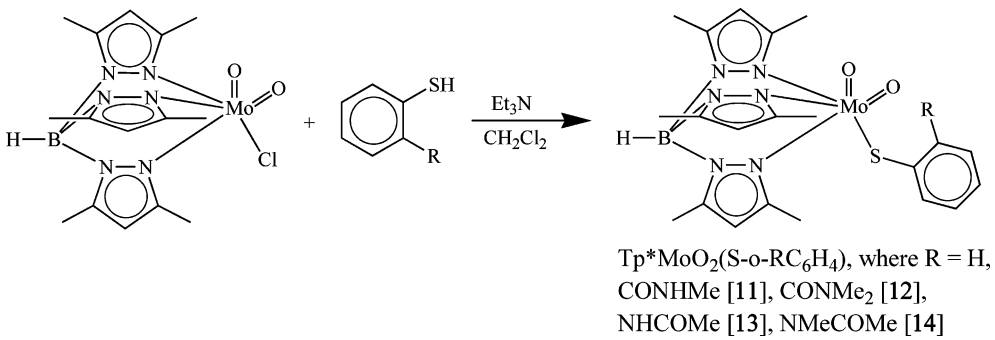

Scheme 2

shows ^{1}H NMR chemical shifts of aromatic protons of thiophenolato ligand in the molybdenum complexes. The doublet resonances (represented as grey bars [red online]) are due to the protons next to the sulfur and the amide substituent, which show upfield shifts upon *N*-methylation, *e.g.* two doublets (a1 and d1) of thiophenol ligand in **11** move from 7.73 and 8.02 ppm (peak separation ~0.29 ppm) to 7.39 ppm (c1) and 7.67 ppm (b1) (peak separation ~0.28 ppm) in **12**. Similar shifts in doublets (a2 and d2) are also observed from **13** to **14**. The NMR chemical shifts are primarily due to electronic effects of substituents and the presence of H-bonding. The substituents containing amide functionality and the corresponding *N*-methylated species have similar electronic coefficients[32] and thus are unlikely to give such a large shift of the NMR signals. Thus, we propose the presence of intramolecular H-bonding in **11** and **13**, which is consistent with solution IR spectra (*vide infra*). The formation of an NH $\cdots$ S hydrogen bond can decrease the electron density on the sulfur atom, which results in a downfield shift of ring protons compared to *N*-methylated complexes where there is no H-bonding present. A larger shift in the pairs of doublets and triplets in **13** to **14** indicates stronger H-bonding compared to **11**, which is again consistent with solution IR-spectra (*vide infra*).

IR spectroscopy. The infrared spectra of the dioxo-Mo(VI) complexes have, due to the *cis*-MoO_2 unit, two strong bands around 924 and 893 cm^{-1} which have been assigned as symmetric and asymmetric vibrational modes respectively. In addition, a sharp B–H stretch is present at 2545 cm^{-1} in all the molybdenum complexes (Table 1). IR bands for amide ν(N–H) and ν(C=O) for **11** and **13** are summarized in Table 2 which also lists similar bands for the corresponding thiols and disulfides. Fig. 4 represents the amide region ν(N–H) and ν(C=O) in the solid-state IR spectra of complex **11** and the corresponding thiol (**5**) and disulfide (**3**). Complex **11** exhibits broad N–H and C=O bands indicating poor crystal packing. Thiol **5** exhibits a slightly larger shift in NH band compared to the disulfide **3**, which is

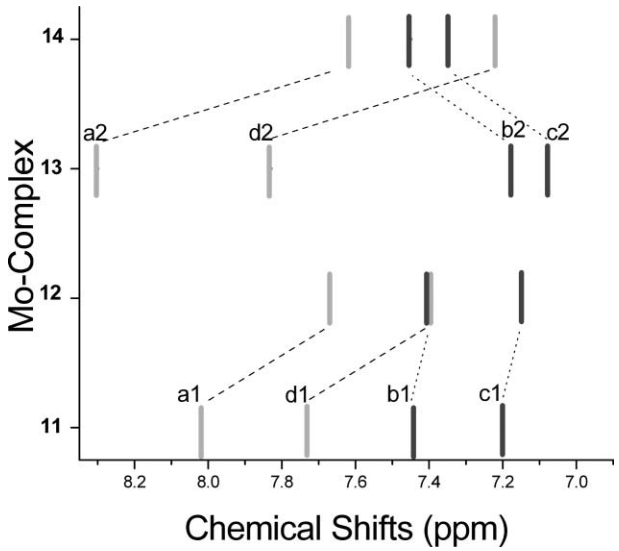

Fig. 3 ^{1}H NMR chemical shifts of the thiophenol phenyl ring in Mo–complexes (black lines [blue online] represent triplet resonances whereas grey lines [red online] represent doublets). All spectra were collected in chloroform-d at room temperature in freshly prepared solutions.

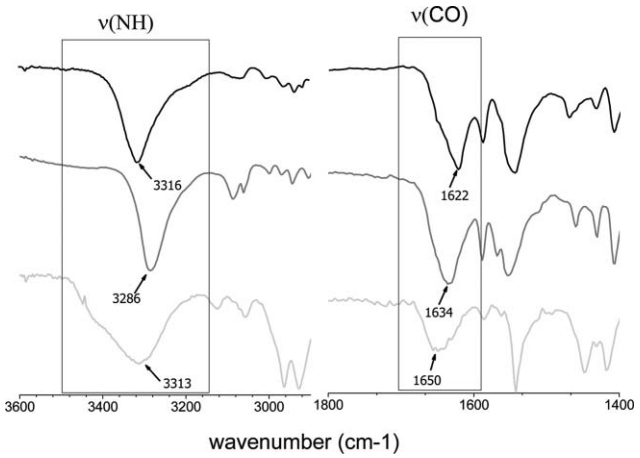

Fig. 4 IR spectra of (top) thiol **5** (on NaCl plate) , (middle) disulfide **3** (in KBr pellet), and (bottom) complex **11** (in KBr pellet).

consistent with 2-^{t}BuNHCOC$_6$H$_4$SH (ν(N–H) ~ 3303 cm^{-1}) and (*S*-2-^{t}BuNHCOC$_6$H$_4$)$_2$ (ν(N–H) ~ 3294 cm^{-1}).[24] The thiol ligands of type A have been proposed to form a SH···O=C H-bond, whereas the thiolato form of the ligand harbors a NH···S H-bonding.[24] In the case of thiol **9**, the ν(N–H) vibration appears at 3202 cm^{-1} and for the corresponding disulfide **7** the ν(N–H) band appears at ~3238 cm^{-1}, opposite to the type A motif described previously. It should be noted that thiol **9** is likely to form intramolecular NH···S hydrogen bonding.[23]

The presence of intramolecular H-bonding in Mo-complexes was examined in solutions of chloroform-d, and the extent of dissociation into ν(N–H$_{bound}$) and ν(N–H$_{free}$) is determined by integrating the intensities of the ν(N–H) peaks of **11** and **13**. Table 2 also summarizes the vibrational frequencies of ν(N–H) and ν(C=O) in the Mo-complexes in solid and in chloroform-d. Both **11** and **13** exhibit two ν(N–H) amide stretching bands in solution compared to a single band in the solid state, indicating the presence of hydrogen-bonded ν(N–H$_{bound}$) and non-hydrogen-bonded ν(N–H$_{free}$) groups as shown in Fig. 5. In the solution state, **11** exhibits two distinct N–H bands at 3325 and 3452 cm^{-1} while in the solid state only one broad N–H band at 3313 cm^{-1} appears.

Table 1 Spectroscopic properties of molybdenum complexes

Complex	Selected IR bands in KBr pellet, ν/cm^{-1}		Electronic spectra in MeCN, λ/nm (ε/M^{-1} cm^{-1})	Redox potential,[a] $E_{1/2}$/V (ΔE_p/V)
	ν(MoO$_2$)	ν(B–H)		
11	893, 924	2549	258 (12980); 403 (2825); 517 (sh, 465)	−1.04 (0.23)
12	890, 924	2553	252 (3580); 407 (970); 520 (sh, 125)	−1.14 (0.24)
Tp*MoO$_2$(SPh)	894, 921	2538	255 (13645); 398 (2350); 519 (sh, 397)	−1.11 (0.12)
13	896, 925	2548	254 (15945); 396 (2785); 504 (sh, 825)	−1.11 (0.12)
14	895, 923	2549	262 (4140); 409 (1225); 526 (sh, 120)	−1.30 (0.15)

[a] In MeCN, room temperature. Scan rate: 0.1 V s^{-1}. Pt-disk working and reference electrodes and a Pt-wire auxiliary electrode; 0.2 M NBu$_4$ClO$_4$ of supporting electrolyte.

Table 2 IR bands of amine and carbonyl stretches

	Disulfide		Thiol		Molybdenum complexes			
	3	**7**	**5**	**9**	**11**		**13**	
	KBr[a]	KBr[a]	NaCl[b]	NaCl[b]	KBr[a]	CDCl$_3$[c]	KBr[a]	CDCl$_3$[c]
ν(N–H)	3284	3238	3315	3202	3313	3325, 3452	3375	3370, 3611
ν(C=O)	1634	1662	1620	1662	1650	1650	1700	1686

[a] KBr pellet. [b] NaCl plate. [c] Chloroform-d solution.

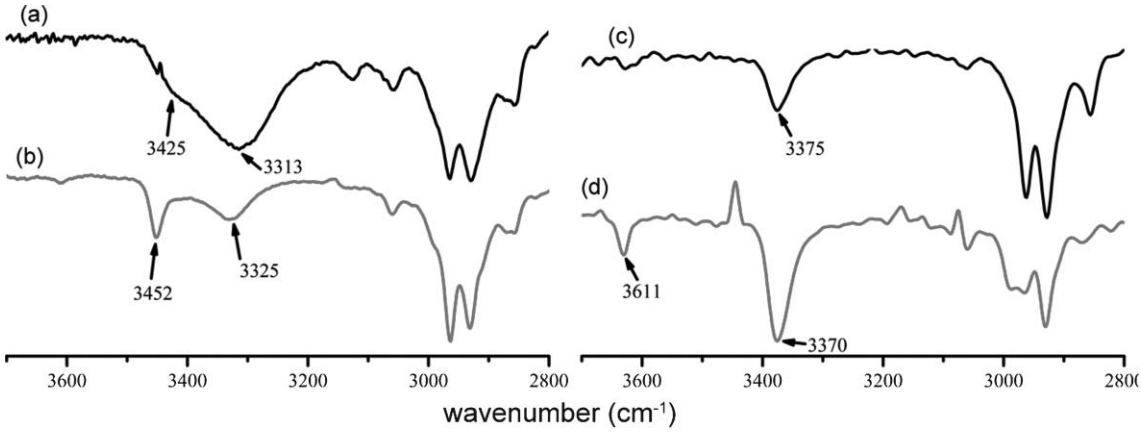

Fig. 5 Comparison of IR spectra in solid and liquid phases: (a) **11** in KBr pellet, (b) **11** in chloroform-d, (c) **13** in KBr pellet, and (d) **13** in chloroform-d. Liquid spectra were recorded using a CaF_2 flow-through cell. (Solution path length = 0.1 mm and concentration ~ 20 mM.)

Thus, in solution the two vibrations are separated by 127 cm^{-1}. Similarly, for **13**, the N–H vibration at 3375 cm^{-1} in the solid state, appears as two bands at 3370 and 3611 cm^{-1} in solution, a separation of 241 cm^{-1}. The N–H···S hydrogen bonds in **11** and **13** are ~26% and ~11% dissociated with respect to the $\nu(N–H_{free})$ forms. Complex **13** shows a larger separation between $\nu(N–H_{bound})$ and $\nu(N–H_{free})$ compared to **11**, by 114 cm^{-1}, indicating stronger N–H···S hydrogen bonding in **13**. This is consistent with the ^1H NMR data described above.

UV-Visible spectroscopy. UV-Visible spectra of dioxo-complexes were recorded in MeCN at room temperature (Fig. 6) and the characteristic band positions are listed in Table 1. A band around 400 nm is due to the S → Mo charge-transfer transition.[33] Interestingly, from **13** to **14**, a red shift of 13 nm was observed due to the absence of intramolecular H-bonding from thiophenolato ligand. Similar electronic effects have also been observed for complexes, **11**, **12**, and **14**, where a blue shift was observed from the electron-donating ligand (NMeCOMe, 409 nm) to the electron-withdrawing group (CONHMe, 403 nm). A shoulder of low intensity around 515 nm is found to be more sensitive to electronic effects. From **13** to **14** the band position shifts from 504 to 526 nm indicating the involvement of intramolecular H-bonding in **13** as discussed earlier. From **11** to **14** the band showed a positive shift of 13 nm. A strong charge-transfer transition around 260 nm can be assigned to the ligand-to-ligand charge transfer. In addition, the intensity of the low-energy transition (*i.e.* ~500 nm) for complexes with H-bonding (**11** and **13**), is higher than that in the *N*-methylated complexes (**12** and **14**). These observations indicate that NHCOMe induces stronger H-bonding than CONHMe.

Electrochemistry

The electrochemical behavior of the Mo-complexes, **11–14**, was studied by cyclic voltammetry along with $Tp^*MoO_2(SPh)$, and the redox potentials are summarized in Table 1. Cyclic voltammograms for all dioxo complexes are shown in Fig. 7, which show one-electron quasi-reversible redox couple, assigned to the Mo^V/Mo^{VI}

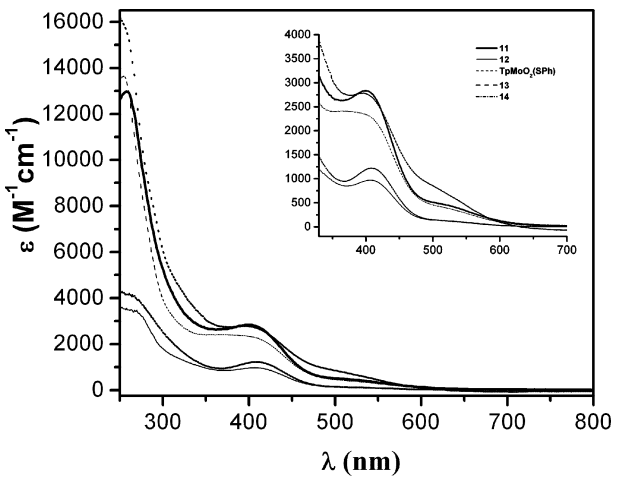

Fig. 6 Electronic spectra of Mo-complexes in MeCN at room temperature.

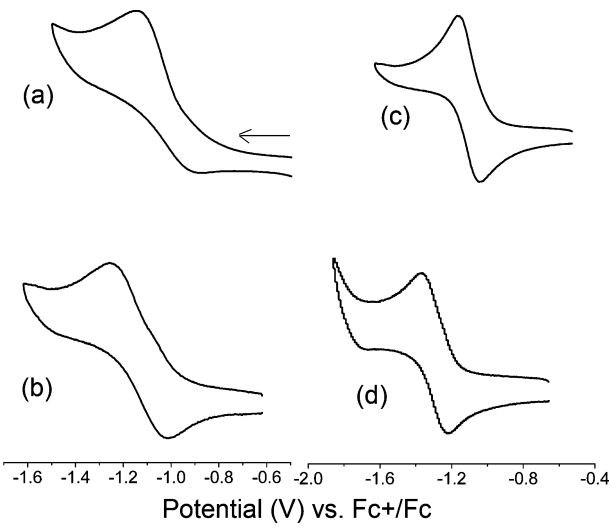

Fig. 7 Cyclic voltammograms of (a) **11**, (b) **12**, (c) **13**, and (d) **14** in MeCN at room temperature. Scan rate: 0.1 V s^{-1}.

process.[30,34] No other reductive response was observed within the solvent window. Consistent with the diffusion-controlled process, the peak currents follow a linear relation with the square root of the scan rate while the half-wave potentials remain independent. Interestingly, the ratios of the peak currents are significantly different from unity, indicating the irreversible nature of the redox couple. Consequently, no attempt was made to generate the corresponding Mo(V) complexes.

The unsubstituted dioxo-Mo(VI) complex, Tp*MoO_2(SPh), also exhibits a one-electron redox couple at −1.11 V *vs.* Fc^+/Fc. Compared to Tp*MoO_2(SPh), the redox potential in complex **11** is shifted by 70 mV in the positive direction, while in complex **13** it is invariant. We interpret the results as **13** having two competing factors influencing the redox potential—an S···H(N) interaction that shifts the potential in the positive direction and the electron-donating effect of the $NHCOCH_3$ group that shifts the potential towards the negative direction. Interestingly, in the case of $[Mo^{V}O(S\text{-}o\text{-}R'CONHC_6H_4)_4]^-$ the Mo(V/IV) couple is shifted towards the positive direction by ~88 mV per ligand with respect to the corresponding *N*-methylated complex.[12] Because each ligand can provide one S···H(N) interaction, 88 mV serves as an estimate for the magnitude of the shift. In the present case, we observe a larger difference in the redox potentials between the compounds with methylated and non-methylated ligands. Thus, redox potentials in **11** and **12** exhibit a difference of 100 mV, while the redox potentials in **13** and **14** are separated by 190 mV. The larger change in **13** compared to **11** indicates a higher strength of the H-bond in the complex, which is consistent with the IR and ^{1}H NMR analyses. Complex **11** is easier to reduce than **13**, even though the CONHMe group is electron-withdrawing and NHCOMe is an electron-donating substituent. The counter-intuitive results reflect the strength of hydrogen bonding.

Conclusion

Dioxo-Mo^{VI} complexes containing *ortho*-substituted thiophenolato ligands have been synthesized and characterized by variety of spectroscopic techniques. Infrared and ^{1}H NMR spectra support the presence of H-bonding in **11** and **13** with a higher strength of H-bonding in **13**. UV-Visible spectra exhibit higher extinction coefficients for complexes harboring intramolecular hydrogen bonding. The electrochemistry of **13** shows a large positive shift in the redox potential compared to the corresponding *N*-methylated complex, **14**. Thus, intramolecular hydrogen bonding with the thiolato sulfur can influence the properties of the metal center. Importantly, the extent of the influence is dependent on the nature of the hydrogen-bonding units present.

Acknowledgements

Financial support from the National Institutes of Health (GM61555) and an equipment grant from the National Science Foundation (CHE 0614785) are gratefully acknowledged. We acknowledge Ms Tina Bhatnagar for preliminary experiments and Ms Eranda Perera for valuable experimental assistance and discussion.

References

1 L. Stryer, in *Biochemistry*, 4th edn, W. H. Freeman, New York, 1995.
2 *Biological Inorganic Chemistry, Structure and Reactivity*, ed. H. B. Gray, E. I. Stiefel, J. S. Valentine and I. Bertini, University Science Books, Sausalito, CA, 2006.
3 C. Kisker, H. Schindelin, A. Pacheco, W. A. Wehbi, R. M. Garrett, K. V. Rajagopalan, J. H. Enemark and D. C. Rees, *Cell*, 1997, **91**, 973–83.
4 N. Schrader, K. Fischer, K. Karsten, R. R. Mendel, G. Schwarz and C. Kisker, *Structure*, 2003, **11**, 1251–1263.
5 E. Karakas, H. L. Wilson, T. N. Graf, S. Xiang, S. Jaramillo-Busquets, K. V. Rajagopalan and C. Kisker, *J. Biol. Chem.*, 2005, **280**, 33506–33515.
6 K. Fischer, G. G. Barbier, H-J. Hecht, R. R. Mendel, W. H. Campbell and G. Schwarz, *Plant Cell*, 2005, **17**, 1167–1179.
7 S. J. N. Burgmayer, Dithiolenes in Biology, in *Dithiolene Chemistry Synthesis, Properties, and Applications*, ed. E. I. Stiefel and K. D. Karlin, 2004, vol. 52, pp. 491–537.
8 R. R. Conry and A. A. Tipton, *JBIC, J. Biol. Inorg. Chem.*, 2001, **6**, 359–366.
9 R. Maiti, K. Nagarajan and S. Sarkar, *J. Mol. Struct.*, 2003, **656**, 169–176.
10 J. J. A. Cooney, M. D. Carducci, A. E. McElhaney, H. D. Selby and J. H. Enemark, *Inorg. Chem.*, 2002, **41**, 7086–7093.
11 K. Baba, T. Okamura, C. Suzuki, H. Yamamoto, T. Yamamoto, M. Ohama and N. Ueyama, *Inorg. Chem.*, 2006, **45**, 894–901.
12 N. Ueyama, T. Okamura and A. Nakamura, *J. Am. Chem. Soc.*, 1992, **114**, 8129–8137.
13 K. Baba, T. Okamura, H. Yamamoto, T. Yamamoto, M. Ohama and N. Ueyama, *Chem. Lett.*, 2005, **34**, 44–45.
14 K. Baba, T. Okamura, C. Suzuki, H. Yamamoto, T. Yamamoto, M. Ohama and N. Ueyama, *Inorg. Chem.*, 2006, **45**, 894–901.
15 J. Huang, R. L. Ostrander, A. L. Rheingold, Y. Leung and M. A. Walters, *J. Am. Chem. Soc.*, 1994, **116**, 6769–6776.
16 K. Baba, T. Okamura, H. Yamamoto, T. Yamamura, M. Ohama and N. Ueyama, *Inorg. Chem.*, 2006, **45**, 8365–8371.
17 (*a*) Representative references include: N. Ueyama, N. Nishikawa, Y. Yamada, T. Okamura and A. Nakamura, *J. Am. Chem. Soc.*, 1996, **118**, 12826–12827; (*b*) T. Ueno, N. Ueyama and A. Nakamura, *J. Chem. Soc., Dalton Trans.*, 1996, 3859–3863; (*c*) N. Ueyama, N. Nishikawa, Y. Yamada, T. Okamura, S. Oka, H. Sakurai and A. Nakamura, *Inorg. Chem.*, 1998, **37**, 2415–2421; (*d*) F-T. Tsai, S-J. Chiou, M-C. Tsai, M-L. Tsai, H-W. Huang, M-H. Chiang and W-F. Liaw, *Inorg. Chem.*, 2005, **44**, 5872–5881.
18 (*a*) S-J. Chiou, C. G. Riordan and A. L. Rheingold, *Proc. Natl. Acad. Sci. U. S. A.*, 2003, **100**, 3695–3700; (*b*) J. N. Smith, Z. Shirin and C. J. Carrano, *J. Am. Chem. Soc.*, 2003, **125**, 868–869; (*c*) J. N. Smith, J. T. Hoffman, Z. Shirin and C. J. Carrano, *Inorg. Chem.*, 2005, **44**, 2012–2017; (*d*) W-Y. Sun, K-B. Zhang and J. Yu, *J. Chem. Soc., Dalton Trans.*, 1999, 795–798; (*e*) M. M. Morlok, K. E. Janak, G. Zhu, D. A. Quarless and G. Parkin, *J. Am. Chem. Soc.*, 2005, **127**, 14039–14050.
19 W-Y. Sun, X-F. Shi, L. Zhang, J. Hu and J-H. Wei, *J. Inorg. Biochem.*, 1999, **76**, 259–263.
20 N. Ueyama, K. Taniuchi, T. Okamura, A. Nakamura, H. Maeda and S. Emura, *Inorg. Chem.*, 1996, **35**, 1945–1951.
21 T. Okamura, S. Takamizawa, N. Ueyama and A. Nakamura, *Inorg. Chem.*, 1998, **37**, 18–28.
22 T. Okamura, N. Ueyama, A. Nakamura, E. W. Ainscough, A. M. Brodie and J. M. Waters, *J. Chem. Soc., Chem. Commun.*, 1993, 1658–1660.
23 M. Kato, T. Okamura, H. Yamamoto and N. Ueyama, *Inorg. Chem.*, 2005, **44**, 1966–1972.
24 M. Kato, K. Kojima, T. Okamura, H. Yamamoto, T. Yamamura and N. Ueyama, *Inorg. Chem.*, 2005, **44**, 4037–4044.
25 T. Okamura, T. Iwamura, H. Yamamoto and N. Ueyama, *J. Organomet. Chem.*, 2007, **692**, 248–256.
26 G. Zuppiroli, C. Perchard, M. H. Baron and C. de Loze, *J. Mol. Struct.*, 1980, **69**, 1–16.
27 J. Huang, R. L. Ostrander, A. L. Rheingold and M. A. Walters, *Inorg. Chem.*, 1995, **34**, 1090–1093.
28 S. A. Roberts, C. G. Young, C. A. Kipke, W. E. Cleland, Jr., K. Yamanouchi, M. D. Carducci and J. H. Enemark, *Inorg. Chem.*, 1990, **29**, 3650–3656.
29 N. Ueyama, T. Okamura, Y. Yamada and A. Nakamura, *J. Org. Chem.*, 1995, **60**, 4893–4899.

30 R. S. Sengar and P. Basu, *Inorg. Chim. Acta*, 2007, **360**, 2092–2099.
31 A. Gryff-Keller and P. Szczeciski, *Magn. Reson. Chem.*, 1985, **23**, 655–658.
32 R. S. Sengar, V. N. Nemykin and P. Basu, *New J. Chem.*, 2003, **27**, 1115–1123.
33 Y. Izumi, T. Glaser, K. Rose, J. McMaster, P. Basu, J. H. Enemark, B. Hedman, K. O. Hodgson and E. I. Solomon, *J. Am. Chem. Soc.*, 1999, **121**, 10035–10046.
34 Z. Xiao, M. A. Bruck, C. Doyle, J. H. Enemark, C. Grittini, R. W. Gable, A. G. Wedd and C. G. Young, *Inorg. Chem.*, 1995, **34**, 5950–62.